Nigerian Journal of Physics (NJP)
ISSN online: 3027-0936
ISSN print: 1595-0611
DOI: https://doi.org/10.62292/njp.v34i1.2025.354
Volume 34(1), March 2025

The Effects of Thermal Annealing on the Electrochemical Performance of Cu -Doped H_3PO_4 Activated Graphite Anode Material for Applications in Batteries

[*1]Matthew, A., [1]Abubakar, A., [1]Ngari, A. Z., [2]Matthew, J., [3]Adoyi, E. and [1]Muhammad, M. S.

[1]Department of Physics, Nigerian Army University Biu, Borno State.
[2]Department of Mathematics, Kaduna State University, Kaduna.
[3]Department of Physics Nigerian Defence Academy Kaduna
[*]Corresponding author's email: alphamatthew4@gmail.com

ABSTRACT

This study utilised the remarkable qualities of graphite that has been activated with H_3PO_4, doped with Cu using the hydrothermal and the drop casting techniques and then annealed at 400 °C and 250 °C in order investigate the electrochemical performance of the composite at these annealing temperatures. To optimise the annealing parameters for advantageous uses in lithium-ion batteries, activating graphite with H_3PO_4, doped with Cu is necessary. Also in the areas of energy conservation and battery innovation, the effects of thermal annealing on the electrochemical characteristics of Copper-doped H_3PO_4 activated graphite anode material are highly relevant. The composite $Cu_{0.1}$:$(H_3PO_4C)_{0.9}$ @ 250 °C ultimately exhibits superior specific capacitance, energy density, and power density, rendering it a more fitting anode material for electrochemical applications. The comparatively higher power density of the $Cu_{0.1}$:$(H_3PO_4C)_{0.9}$ @ 400 °C sample is mostly explained by its lower equivalent series resistance. The GCD characterization results, which indicated that Cu^{2+} insertion (which causes the voltage to decrease) and extraction (which causes the voltage to increase) into and out of the H_3PO_4C anode are the primary causes of the changes in the charging voltage, and is supported by the cyclic voltammetry results, which demonstrate that redox currents are only set up in this voltage range with an oxidation peak around 0.6 V.

Keywords:
Annealing,
Anode,
Battery,
Density,
Electrode,
Energy,
Graphite,
Power.

INTRODUCTION

Graphite has garnered considerable interest as a potential high energy density, enhanced electrochemical and an efficient anode component for lithium-ion batteries (Smith *et al*., 2018). Copper is a necessary dopant in this anode material that affects its electrochemical characteristics. According to Zhang and Wu's (2017) research, the annealing process significantly alters the spatial distribution of the copper molecules inside the graphite matrix, hence influencing the conductivity as well as the electrochemical capacity of the material. One of the issues this research attempts to address was the comprehension of how and to what degree thermal annealing could modify the electrochemical performance of graphite anode materials in batteries. Lithium-ion batteries (LIB) offer high gravimetric and volumetric energy densities which renders them particularly suitable for electronic applications. In order to optimize their performance, in particular with larger energy density, there is a continuous search for novel electrode materials. Electrode materials based on conversion and doping mechanisms promise extremely enhanced electrochemical capacities in lithium-ion batteries as compared to conventional materials (Aravindan *et al*., 2015: Mahmood *et al*., 2016). However, high energy densities of actual electrodes as well as high surface areas are relevant issues to be considered. High reactivity associated with high surface area typically promotes reversible processes in associated electrolyte consumption. In this respect, due to carbon's restricted voltage regime of electrochemical activity (Goriparti *et al*., 2016), activated graphite is a valuable material to protect active nanomaterials, thereby avoiding enhanced electrolyte degradation and associated gas production. A key factor required in studying the electrochemical characteristics of copper-doped H_3PO_4 activated graphite anode material is thermal annealing. The crystallinity, copper transportation, and electrochemical performance of the material can all be improved by selecting the right annealing conditions. To optimise the annealing parameters for advantageous uses in lithium-ion batteries, more study is necessary. In the areas of energy conservation and battery innovation, the effects of thermal annealing on the electrochemical characteristics of Copper-doped H_3PO_4 activated graphite anode material are highly relevant. By comprehending how thermal annealing affects these characteristics, better anode materials with increased reliability and durability can be fabricated. With this information, the annealing settings may be optimised and the material's characteristics, such its high energy density and long cycle life, can be tailored to fit the needs of certain applications. In the end, the creation of stable and effective anode materials can aid in the progress of renewable energy sources, lessen dependency on fossil fuels, and encourage a more environmentally friendly and sustainable economy.

MATERIALS AND METHODS

Synthesis Cu doped H_3PO_4 activated Graphite composite

20 g of the graphite (99 %), 0.1 mol/L copper sulphate, and 1000 ml of distilled water and 6.7 ml of 86% phosphoric acid (H_3PO_4) was added to 1000 ml of distilled water and then stirred using magnetic stirrer for 3 hours to obtain a composite. The composite was then filtered, after which the mixture was sonicated at 78.8 °C for 3 hours. After sonication the sample was then dried in an electrical oven at 75 °C for 3 hours. The sample was then grinded into a fine powder using piston and mortar to obtain the composite material $Cu_{0.1}:(H_3PO_4C)_{0.9}$. The composites material was then annealed at 250 °C and 400 °C using Muffle furnace, model SX-2.5-10.

Preparation of Composites for Electrochemical Characterisation

In the preparation of the composite material for characterisation, a stainless-steel substrate was used. The substrate was first smoothened after which it was washed with distilled water. The substrate was then soaked in an acetone for 1 hour before washing again with distilled water, after which it was ultrasonicated for 30 minutes and then dried in an electric oven for 1 hour. 90% sample powder, 10% polyvinylidene flouride (PVDF) binder were dissolved in N-methylpyrrolidone (NMP) and stirred for 5 hours until it formed slurry. It was then loaded uniformly on the treated stainless steel substrate. After deposition, it was then dried in an electric oven at 120°C for 5 hours. The electrode is formed and ready for characterisation.

RESULTS AND DISCUSSION

Cyclic Voltammetryand EIS Analysis

The values of specific capacitance (C_{sp}), energy density (E_D) and power density (P_D) were calculated using the equations below;

$$(C_{sp}= \frac{S}{2mk(E)}, \boldsymbol{E_D} = \frac{1}{4}C_{sp}V^2 \text{ and} \boldsymbol{P_D} = \frac{1}{4X(ESR)}\frac{V^2}{M})$$

Where $C_{sp}$is the specific capacitance, S is the integral charge surface area of the CV curve in (AV), m is the mass of the electrode material in (g), k is the scan rate in (mV/s) and E is the value of the electrode potential in (V). The EIS measurement was done within the explored frequency range of 100,000 to 0.1 Hz.

The summary of the results from the electrochemical analysis for the $Cu_{0.1}:(H_3PO_4C)_{0.9}$composite @ 250 °C annealing temperature and $Cu_{0.1}:(H_3PO_4C)_{0.9}$ composite @ 400 ^{0}C annealing temperature at scan rate of 5 mVs^{-1} are given in Table 1

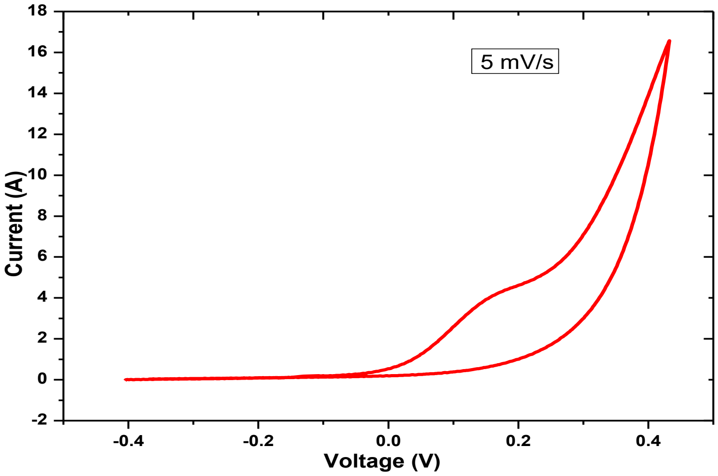

Figure 1: Cyclic Voltamogramm curve at different scan rates for $Cu_{0.1}:(H_3PO_4C)_{0.9}$ composite electrode @ 250 °C annealing temperature

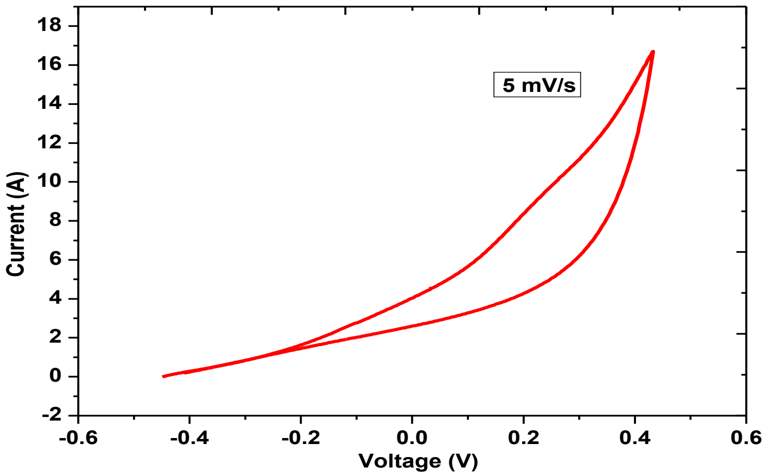

Figure 2: Cyclic Voltamogramm curve at different scan rates for $Cu_{0.1}$:$(H_3PO_4C)_{0.9}$ composite electrode @ 400 ºC annealing temperature

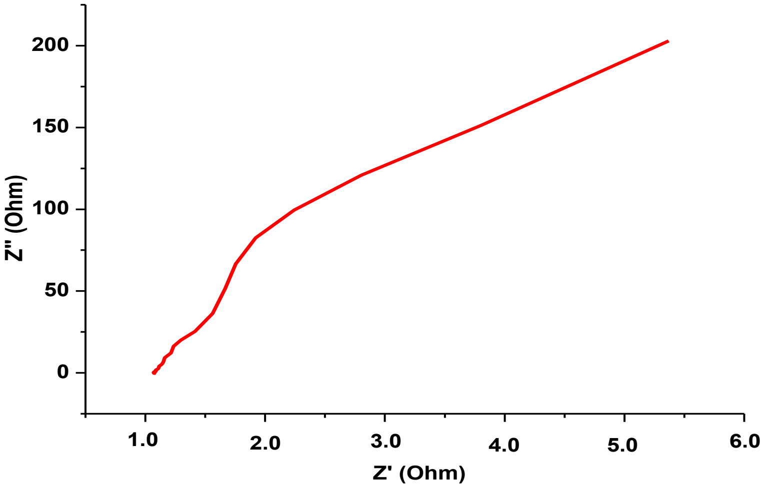

Figure 3: EIS Plot for $Cu_{0.1}$:$(H_3PO_4C)_{0.9}$@ 250 ºC annealing temperature

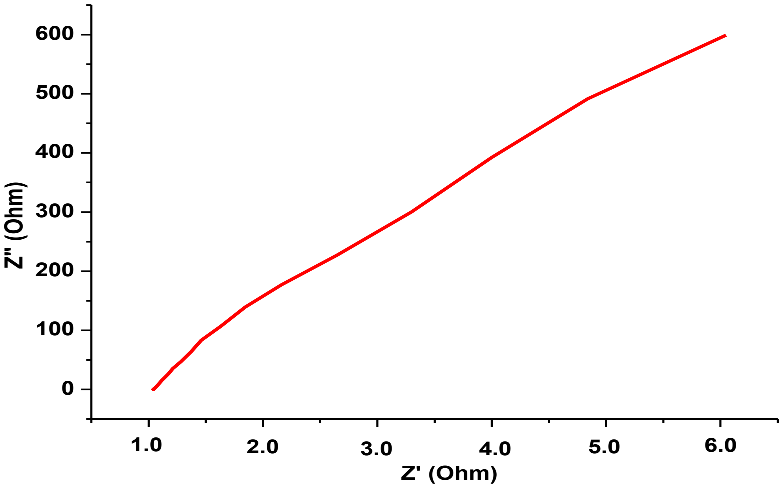

Figure 4: EISPlot for $Cu_{0.1}$:$(H_3PO_4C)_{0.9}$@ 400 ºC annealing temperature

Table 1: The Values of C_{SP} and E_D and P_D @ 5mV/s

S/N	Composite	Mass (g)	Potential (V)	ERS (Ω)	C_{sp}(F/g)	E_D (Wh/kg)	P_D (W/g)
1	$Cu_{0.1}$:$(H_3PO_4C)_{0.9}$ @ 400°C	0.11	0.6	0.48	1974.94	49.37	1.70
2	$Cu_{0.3}$:$(H_3PO_4C)_{0.7}$@ 250°C	0.11	0.6	0.40	5445.85	306.33	2.05

The CV curves of different samples obtained at a scan rate of 5 mVs^{-1} between 0.0 and 0.6 V are shown figures (1 and 2) only one pair of redox peaks corresponding to the extraction/insertion of copper from/into the lattice of the H_3PO_4C. Furthermore, because the CV curves for the cycles are almost very similar, copper insertion/extraction to/from the H_3PO_4C sample is thus highly reversible. The anodes material shows a high irreversible capacity loss, and this phenomenon may be attributed mainly to the side reactions, such as the formation of solid electrolyte interface (SEI), copper adsorption in the conductive additive carbon black (graphite), and irreversible electrochemical decomposition of the electrolyte, this clearly agrees with the work of (Lan *et al.*, 2017). The composites $Cu_{0.1}$:$(H_3PO_4C)_{0.9}$ @ 250 °C give a higher specific capacitance, energy density and power density, thereby making it a more suitable anode material when used in electrochemical applications. The sample $Cu_{0.1}$:$(H_3PO_4C)_{0.9}$ @ 400 °C has a relatively higher power density.

GCD Characterisation

The cyclic voltammetry results, which show that redox currents are only set up in this voltage range with an oxidation peak around 0.6 V, support the GCD characterization results, which indicate that the change in the charging voltage is primarily caused by Cu^{2+} insertion (the voltage decreases) and extraction (the voltage increases) into and from the H_3PO_4C anode. Fast changes in the concentration of Cu ions in the lamellar planes of the H_3PO_4C structure are implied by high currents, which also suggest quick changes in the anode voltage in a brief amount of time. As shown in tables 2 and 3, the amount of charge stored in the anode material during charging is represented by a linear reduction in charge capacity with increasing charging current intensity as seen in figures 5 and 6. Ionic polarisation, whose value is proportional to the current intensity, is the primary cause of the observed decrease in the charge and discharge capacities at the current density of 5 A/g.

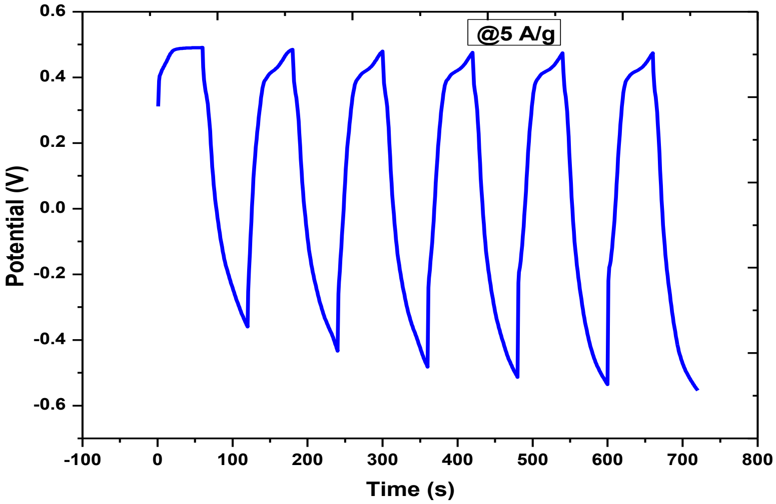

Figure 5: Shows the galvanostatic charge discharge GCD pattern for sample $Cu_{0.1}$:$(H_3PO_4C)_{0.9}$ composites @ 250 °C annealing temperature

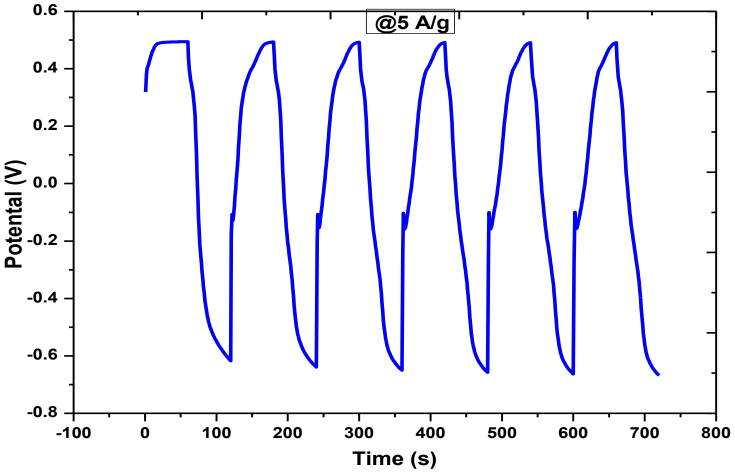

Figure 6: shows the galvanostatic charge discharge GCD pattern for sample $Cu_{0.1}$:($H_3PO_4C)_{0.9}$ composites @ 400 ºC annealing temperature

.

Table 2: Values of C_{SP} and E_D for $Cu_{0.1}$:$(H_3PO_4C)_{0.9}$ @5A/g, @250 ºC and 0.6 V for GCD

	First cycle	Second cycle	Third cycle	Fourth cycle	Fifth cycle	Sixth cycle
ΔT	76.95	61.13	58.91	54.06	53.03	52.98
ΔV	0.84	0.91	0.93	0.98	0.98	0.98
C_{SP}	458.03	335.87	300.56	275.81	270.56	265.45
E_D	80.79	72.16	69.53	66.22	64.96	63.73

Table 3: Values of C_{SP} and E_D for $Cu_{0.1}$:($H_3PO_4C)_{0.9}$ @5A/g, @400 ºC and 0.6 V for GCD

	First cycle	Second cycle	Third cycle	Fourth cycle	Fifth cycle	Sixth cycle
ΔT	79.26	64.07	64.00	54.91	53.15	53.06
ΔV	0.84	0.91	0.93	0.98	0.98	0.98
C_{SP}	384.75	273.49	269.18	242.96	235.15	224.77
E_D	102.04	90.49	90.39	77.55	75.06	74.94

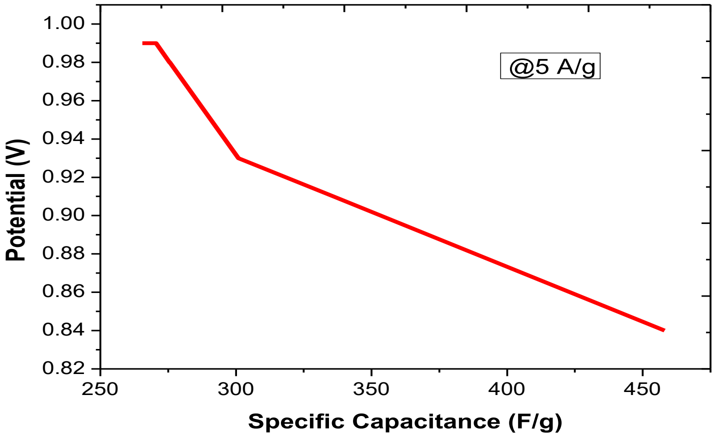

Figure 7: Capacity retention for $Cu_{0.1}$:($H_3PO_4C)_{0.9}$ composites @ 400 ºC annealing temperature

.

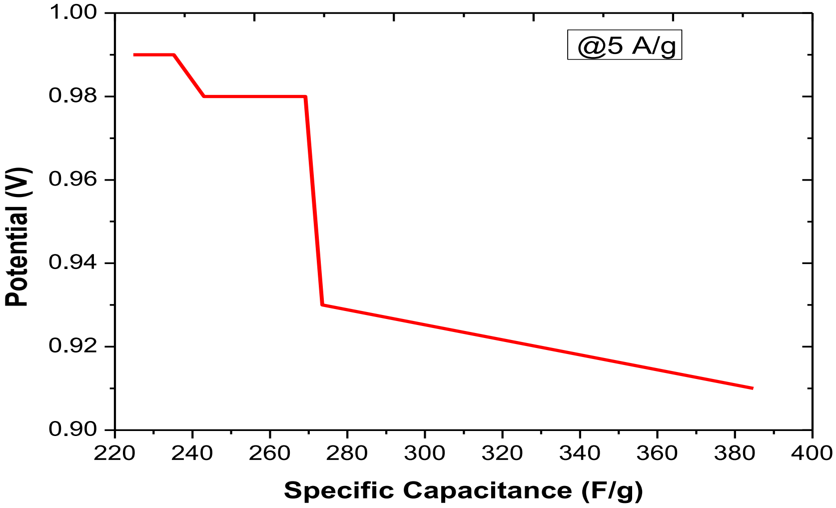

Figure 8: Capacity retention for $Cu_{0.1}$:($H_3PO_4C)_{0.9}$ composites @ 400 °C annealing temperature

CONCLUSION

This study showed that, the composite $Cu_{0.1}:(H_3PO_4C)_{0.9}$ @ 250 °C ultimately exhibits superior specific capacitance, energy density, and power density, rendering it a more fitting anode material for electrochemical applications. The comparatively higher power density of the $Cu_{0.1}:(H_3PO_4C)_{0.9}$ @ 400 °C sample is mostly explained by its lower equivalent series resistance. The GCD characterization results, which indicated that Cu^{2+} insertion (which causes the voltage to decrease) and extraction (which causes the voltage to increase) into and out of the H_3PO_4C anode are the primary causes of the changes in the charging voltage, and is supported by the cyclic voltammetry results, which demonstrate that redox currents are only set up in this voltage range with an oxidation peak around 0.6 V.

REFERENCES

Adesina, G.T., Kovo, A.S., and Abdulhamid, M.A. (2021). Effect of Thermal Annealing on the Structural and Electrochemical Properties of Aluminium Doped K_2CO_3 Activated Coconut Husk Carbon-Based Composites. *Journal of Materials Science and Chemical Engineering*, vol. 9, pp. 19-32.

Aravindan, V., Lee, Y.S., and Madhavi, S. (2015). Research Progress on Negative Electrodes for Practical Li-Ion Batteries: Beyond Carbonaceous Anodes. *Adv. Energy Mater*. 5, 1402225,. https://doi.org/doi:10.1002/aenm.201402225 .

Ali, A., Liang, F., Zhu, J., & Kang, P. (2022). The role of graphene in rechargeable lithium batteries : Synthesis , functionalisation , and perspectives Nano Materials Science The role of graphene in rechargeable lithium batteries : Synthesis , functionalisation , and perspectives. *Nano Materials Science*, *August*. https://doi.org/10.1016/j.nanoms.2022.07.004

Alpha, M., Uno, U.E., Isah, K.U., and Ahmadu, U. (2019).Structural and Electrochemical Properties of Ag_xSnO_{1-x}/G ($0.3 \leq \times \leq 0.4$) Composite Electrode. *European Journal of* Scientific *Research*, vol. 151, pp. 479-488. http://www.european journal of scientific research.com

Ahmad, M.A., Ahmad, N., and Yusoff, A.R. (2016). Potassium hydroxide activated carboderived from coconut husk as a high-performance adsorbent for methylene blue. *Ecotoxicology and environmental safety*, vol. 134, pp. 338-345.

Chen, J., Wu, K., Li, W., Chen, K., Cao, D., and Luo, X. (2019). Synthesis of Al_2O_3/K_2CO_3- modified activated carbon derived from coconut husk by microwave-assisted method for high-performance supercapacitors. *Ceramics International*, vol. 45(16), pp. 20476-20486.

Diantoro, M., Rahmadani, H., and Maharani, T. (2024). Microsructure and Electrochemical Performance of Supercapacitor Based on Nickel/Activated Carbon Composite Electrode. *Journal of Physics: Conference Series*, vol. 2734, pp. 01201.

Fangli, Z., Wenchao, Z., David, W., and Zaiping, G. (2022). Recent progress and future advances on aqueous monovalent-ion batteries towards safe and high power energy storage. *Advanced Materials*, vol. 34, 2107965.

Goriparti, S., Miele, E., de Angelis, F., Di Fabrizio, E., Proietti Zaccaria, R., Capiglia, C. (2016). Review on recent progress of nanostructured anode materials for Li-ion batteries. *J. Power Sources* 257, 421–443, https://doi.org/doi:10.1016/j.jpowsour.2013.11.103 .

Kumar, M., Somanathan, T., and Parthasarathy, S. (2019). Activated carbon from coconut shell as electrode material for supercapacitors, *Journal of Electrochemical Science and Engineering*, vol. 9(2), pp. 103-112.

Lan, H., Qian, S., and Wang, Q. (2017). $Sr_{1-x}Na_{2x}Li_2Ti_6O_{14}$ ($0 \leq x \leq 1$) as anode materials for rechargeable Li-ion batteries. *Ceramics International*, vol. 43, pp. 1552-1557.

Mahmood, N., Tang, T., Hou, Y. (2016). Nanostructured Anode Materials for Lithium Ion Batteries: Progress, Challenge and Perspective. *Adv. Energy Mater*. 6, 1600374, https://doi.org/doi:10.1002/aenm.201600374

Shichen, Y., Yangyang, F., Jing, L., and Yaobing, W. (2023). Metal-Oxide Bicatalysis Batteries for Energy Storage and Chemical Production. *Advanced Materials*, vol. 35(40), pp. 221-227.

Singh, P., Rawat, K.S., Chauhan, D.S., Poddar, P., and Kim, K.H. (2021). Activated coconut husk carbon-based composite for high-performance supercapacitor electrode applications. *Chemical Engineering Journal*, vol. 405, pp. 126937.https://doi.org/10.1016/j.cej.2020.126937

Wang, X., Gao, G., Li, Y., Chen, H., and Ding, X. (2020). Self-healing supercapacitor with high performance based on a hydrogel composite. *Journal of Materials Chemistry A*, vol. 8(6), pp. 3373381, 2020.

Yu, M., Li, R., Wu, M., & Shi, G. (2015). Graphene Materials for Lithium − Sulfur Batteries Graphene materials for lithium – sulfur batteries. *Energy Storage Materials*, *1*(January 2019), 51–73. https://doi.org/10.1016/j.ensm.2015.08.004

Yan, L., Fang, L., Zhang, Y., Hao, X., and Sun, X. (2020). Enhanced Li+ ion transference number of Al-doped K_2CO_3 solid electrolyte via rational design. *Journal of Materials Science:Materials in Electronics,* vol. 31, pp. 7242-7251.

Zhao, H., Xu, Z., Zhang, L., Liu, Y., and Che, F. (2020). Modified coir-based activated carbon for enhanced removal of methylene blue: Preparation, characterization and adsorption properties. *Journal of Environmental Chemical Engineering*, vol. 8, pp. 104083. https://doi.org/10.1021/acscentsci.0c00449

Zhang, H., Cao, J., Chen, X., Wang, J., Bian, K., and Yuan, H. (2019). Rational design and synthesis of K_2CO_3: Al_2O_3 solid electrolytes with high ionic conductivity for lithium ion batteries. *Journal of Energy Chemistry*, vol. 38, pp. 67-73.

Zhang, H., Bian, K., Yang, W., Wang, J., Li, X., and Yuan, H. (2017). Ionic conductivity improvement of K_2CO_3:Al_2O_3 solid electrolyte with a high Al content for lithium-ion batteries. *Electrochimica Acta*, vol. 238, pp. 246-253.

Zhang, Q., Zhang, B., Ma, S., Wang, R., Zhu, C., and Zhao, X.S. (2020). Preparation and Evaluation of Coconut Shell-Based Activated Carbon with High Performance as Supercapacitor Electrode Materials. *Journal of Energy Storage*, vol. 31, pp. 101651, 2020.